

## The astronomical photometric data and its reduction procedure

Gireesh C. Joshi

P.P.S.V.M.I. College, Nanakmatta, U.S. Nagar-262311, Uttarakhand, India

---

**Abstract:** *The photometric data reduction procedure is the fundamental step to get the signal information of stellar objects. These signals are collected through the CCD camera; the brief notes have been given about the character and work function of the CCD camera. Here, we are briefly discussing about the reduction procedure of the UBVRI photometric system, which is worldwide utilizing for stellar study from last two or three decades. Moreover, the procedure of standardization has been given for the captured CCD images. Presently, there are several databases/catalogues, which are supplemented by the various surveys; these databases are effective to analysis the properties of any interested stellar objects. The associated web-service of these databases/catalogues is effective to improve the scientific knowledge of the Society, and provide an opportunity to study of the stellar dynamics and associated evolution. We have been listed their brief information and importance in the Scientific Society. These topics are a basic need for the any comprehensive study of stellar astronomy.*

**Keywords:** *Astronomy: photometric methods – database – telescopes – astronomical reduction – statistical analysis*

---

### I. Introduction

The Earth is a spec of dust on the astronomical scale; astronomy contains the physics of several stellar objects. These objects are very far away from Earth; moreover, they are the most interested and attractive objects for human beings. Human beings are continuously developing and installing the observational facilities (telescopes) for solving the mystery of the Universe. The various photometric bands/filters are associated with these telescopes, and each band show different effective wavelength to detect the information about the interior physical phenomenon. The detected information can be used to constrain the dynamism and evolution model of interested stellar objects. Heavier atoms of matter are to be made in the interior part of stars and prescribed matter to pervade into space through the “Supernova burst”. Our earth is also made of such type materials. Thus, every molecule of our bodies is contained the matter that once was subjected to the tremendous temperatures and pressures at the center of a star (Harwit, 2006). As a result, the iron in our blood, required oxygen of our breath, carbon, nitrogen, etc. of our tissues and calcium in our bones was formed through the fusion of smaller atoms at the center of a star. There are the several theories for explaining the formation of the planets, stars and other astronomical objects. These theories are guide to us for understanding the truth of formation of the Universe, but these are not truth itself (Harwit, 2006). Consequently, these said theories are continuously revised and to keep leading us in the right direction. The astrophysics is a deeper understanding of the Universe and the information about the evolution of the Universe is continually increased through the analysis of new collected data. Moreover, this information is further leading the new concepts/models for describing the our present Universe and its future. Other words, the astrophysics are a scientific branch to understand the formation of planets, stars, pulsars, galaxies etc. and their associated physical phenomenon. The revolutionary changes has been occurring in the literature of astrophysical study due to the incorporation of new technology and algorithms. In the 19th and 20th centuries, the astronomical studies had been carried out through the photoelectric and photographic data. The astronomical data had been collected through the various ground based observatories and space missions. The seeing conditions are highly influenced these observations, which leads the resolution and image quality of the instrument. Since, the accurate analysis is highly dependent on the quality of the data, therefore the ground based observations are performed at the time of stable weather conditions and cloud free sky. Recently, the photometric study of astronomical objects is carried out through the charged-couple-device (CCD) cameras.

#### 1.1. Charge-couple devices

A silicon chip contained an array of light sensitive diodes, used for capturing images. The photodiodes, arranged in an array of rows and columns, become charged when light falls on them. The amount of charge depends on the amount of light, which may be built up over time. These charges are read out column by column to provide an analogue signal of the image in the array, which is then converted to digital form for display and storage on a computer. CCDs are widely used both by professional and amateur astronomers as they are more sensitive to light than a photographic emulsion, give an output in almost constant proportion to the amount of

light falling on them (i.e. a linear response), and have no reciprocity failure. The image can be displayed almost immediately after the end of the exposure, and image processing can be used to enhance it. However, the detector area is much smaller than a photographic plate or film, which can be of any size required and provides much finer resolution. In the year 1975, the Scientists from the Jet Propulsion Laboratory were imaged first astronomical CCD image of the planet Uranus at a wavelength of 8900 Å (Janesick & Blouke, 1987). The CCD is made by a solid-state electronic component, which is a small rectangular piece of silicon wafer. This wafer is an array of individual light sensitive tiny picture element and said element is defined as a pixel. The said CCD cameras are containing their special and sensitive characteristics such as low noise for long exposure time, large quantum efficiency, linearity, extended spectral sensitivity, image processing possibilities, real time aspect etc. In the present day CCDs generally come in sizes ranging from 512 by 512 picture elements or pixels to arrays as large as 8192 by 8192 pixels (Howell, 2006). The read-noise and gain are the main characteristics of these CCDs cameras. Noise is arisen due to the collection of electrons and the transfer of charge packets. During the collection of electrons, noise stems from thermal processes, light pollution and the generation of electron-hole pairs in the depletion region (Burt, 1974; Kristian et al., 1982; Weisner & David, 1992). To minimize the effect of thermal noise, CCD is cooled to very low temperatures, which are typically around 150-160 K (Kristian et al., 1982). In this low temperature, the work function of CCD is known as the slow scan mode, which permits long exposures of up to several hours (Weisner & David, 1992). Similarly, the heater and artificial light sources must be closed at the time of the observations of astronomical objects, which is further needed to reduce the thermal noise.

### **1.2. Working operation of CCD**

CCD is based on the principal of photoelectric effect and also performs four tasks to generate an image namely photoelectron generation, electron collection, charge transfer and analog to digital read out. The each pixel of CCD array is a tiny detector for the photons of incident light. The incident photons hit the pixel region of silicon chip and these photons are absorbed by the electrons of the hitting area. These electrons are excited and freely move towards to the conduction band due to the extra absorbed energy of the photon compare to work function of metal surface. The photons having energy 1.1 to 4 eV generate single electron-hole pairs, whereas those of higher energy produce multiple pairs. Each individual pixel is collect the photons and store the produced electrons by these photons. These said electrons can be read out from the CCD array to a computer, which lead to produce a digital image of varying intensities of light detected by the CCD. In this connection, the electrons build up in the wells (pixels) over the period of its exposure to light (the integration) due the contact of incident photons with the CCD surface. A digital image is built up consisting of the pattern of electrical charge (intensity) present in each pixel. At the end of integration period, the incident light does not reach the CCD detector and the accumulated charge in each pixel is transferred to the on-chip amplifier, pixel by pixel. During the read out process, charge from the array must be moved out of the imaging region to a location where the amount of charge can be measured. The information from the rows of pixels is move down to a single parallel row (the serial register) which is read out sequentially by Analog-to-Digital (A/D) converter where it is measured and then recorded. The said collected charge of each pixel is measured in the form of voltage. This voltage is converted into digital number by A/D converter. The prescribed measuring device is emptied and once again the process is repeated. This process continues until all of the pixels have been measured (read out). On this background, an electronic map of the optical image which matches with the photons of the CCD saw is recreated at the computer.

### **1.3. Features and parameters of the CCD images**

The sampling parameter ( $r$ ) of a source of the CCD image is defined as (Howell et al., 1996; Buonanno & Iannicola, 1989),

$$r = \frac{FWHM}{p},$$

where  $FWHM$  is the full-width half-maximum value of the source PSF and  $p$  is the pixel size, both values given in the same units. If the value of  $r$  is less than 1.5 then digital data are considered under sampled and such values are obtained for very good seeing sites, adapting optics system and CCD images obtained outside the Earth's atmosphere i.e., space-based telescopes (Howell, 2006). The said under sampled images are produced by a typical wide-field telescope outfitted with a large-format CCD, such as a Schmidt telescope or a camera lens, or a space-based telescope such as the Hubble Space Telescope wide-field planetary camera (WFPC) (Holtzman, 1990; Howell et al., 1996). The signal to noise ratio (S/N) of a CCD image is computed through the following equation (Mortara & Fowler, 1981),

$$\frac{S}{N} = \frac{N_*}{\sqrt{N_* + n_{pix}(N_S + N_D + N_R^2)}}$$

where  $N_*$ ,  $n_{pix}$ ,  $N_S$ ,  $N_D$  and  $N_R^2$  are the total number of photons (signal) collected from the object, the number of pixels under consideration for the S/N calculation, the total number of photons per pixel from the background or sky, the total number of dark current electrons per pixel and the total number of electrons per pixel resulting from the read noise respectively.

## II. Observational data and equipment

The astronomical observations of optical and infrared windows are collected through a set of instruments (telescope mirror, filters and detectors etc.). These instruments are collected and concentrated the stellar radiation at focus point/plane of the telescope. Astronomers are collected useful information through the analysis of these observations and also supplied these information to other researchers for further analyzing. The various important astronomical data-sets are available in various catalogues such as SIMBAD<sup>1</sup>, ESO Online digital Sky Survey, VIZIER SERVICE, WEBDA<sup>2</sup> etc.

### 2.1. Database

The databases are compiled through the photometric survey and studies. Such type data have led to many discoveries in several areas of modern astronomy: asteroseismology, exoplanets and stellar evolution (Huber et al., 2012; De Medeiros et al., 2013; Walkowicz & Basri, 2013; Paz-Chinchon et al., 2015). The efficiency of a large-area survey can be estimated by the Metric,

$$\epsilon = \Omega D^2 q$$

where  $\Omega$  is the solid angle of the field of view, D is the diameter of the telescope, and q is the total throughput quantum efficiency of the instrument assuming that the seeing disk is resolved (Howell, 2006).

#### 2.1.1. arXiv

The arXiv (pronounced "archive", "X" were used instead of the Greek letter Chi,  $\chi$ ) is a repository of electronic preprints, known as e-prints, of scientific papers in the fields of mathematics, physics, astronomy, computer science, quantitative biology, statistics, and quantitative finance, which can be accessed online. In many fields of mathematics and physics, almost all scientific papers are self-archived on the arXiv. Begun on August 14, 1991, arXiv.org passed the half-million article milestone on October 3, 2008, (Ginsparg, 2011) and hit a million by the end of 2014 (Vence, 2014; Staff, 2015). By 2014 the submission rate had grown to more than 8,000 per month (Staff, 2015). The arXiv was made possible by the low-bandwidth TeX file format, which allowed scientific papers to be easily transmitted over the Internet and rendered client-side (O'Connell, 2000). Presently, It is hosted principally by Cornell, with 8 mirrors around the world. Although the arXiv is not peer reviewed, a collection of moderators for each area review the submissions; they may recategorize any that are deemed off-topic (McKinney, 2011), or reject submissions that are not scientific papers. Under the system, an author must be endorsed by an established arXiv author before being allowed to submit papers to require categories. Endorsers are not asked to review the paper for errors in the submitted manuscript, but to check whether the paper is appropriate for the intended subject area (McKinney, 2011). The endorsement system has attracted criticism for allegedly restricting scientific inquiry (Greechie et al., 2005). This prescribed "endorsement" system was introduced in 2004 as part of an effort to ensure content that is relevant and of interest to current research in the specified disciplines (Ginsparg, 2006). The arXiv does contain some dubious e-prints, such as those claiming to refute famous theorems or proving famous conjectures using only high-school mathematics, they are "surprisingly rare" (Jackson, 2002). This service is very effective to obtain the scientific draft of authors, which are payable in the journal. in addition, the context of these draft can used to the scientific improvement of the algorithm of the researchers.

<sup>1</sup><http://simbad.u-strasbg.fr/guide/index.htm>

<sup>2</sup><https://www.univie.ac.at/webda/>

### **2.1.2. Astronomical data system**

The Astrophysics Data System (ADS) is developed by the National Aeronautics and Space Administration (NASA). Moreover, it is an online database of over eight million papers (related to astronomy and physics) from both peer reviewed and non-peer reviewed sources. Abstracts of almost all articles are available to us in the form of free online. In addition, full scanned articles such as Graphics Interchange Format (GIF) and Portable Document Format (PDF) of older articles are available in the service of ADS. New articles have links to electronic versions hosted at the journal's webpage, and these are typically available only by subscription (which most astronomy research facilities have). It is managed by the Harvard Smithsonian Center for Astrophysics. ADS is a powerful research tool and has had a significant impact on the efficiency of astronomical research since it was launched in 1992. Literature searches that previously would have taken days or weeks can now be carried out in seconds via the ADS search engine, custom-built for astronomical needs. Studies have found that the benefit to astronomy of the ADS is equivalent to several hundred million US dollars annually, (Kurtz et al., 2000) and the system is estimated to have tripled the readership of astronomical journals (Kurtz et al., 2005).

### **2.1.3. VizieR**

VizieR is a database grouping in an homogeneous way thousands of astronomical catalogues gathered for decades by the Centre de Données de Strasbourg (CDS) and participating institutes (Ochsenbein et al., 2000). The Centre de Données astronomiques de Strasbourg (CDS) has a very long experience in acquiring, cross-identifying, and distributing astronomical data (Genova et al., 2000). VizieR has become a reference point for astronomers worldwide engaged in research, who come to access catalogued data regularly published in astronomical journals. The new VizieR service was refurbished in 1997 by the CDS to better serve the community in terms of searching capabilities and data volume. As of March 2012 it contains more than 9800 catalogues. VizieR is an illustration of the benefits resulting from a homogeneous documentation of the existing astronomical catalogues, facilitating the transformation of a set of heterogeneous data into a fully interactive database, furthermore able to interact with remote services (Ochsenbein et al., 2000).

### **2.1.4. SIMBAD**

Simbad was created by merging the catalog of Stellar Identifications (CSI, Ochsenbein et al. (1981)) and the Bibliographic Star Index (Ochsenbein, 1982). SIMBAD is an astronomical database of objects beyond the Solar System. It contains identifications, "basic data", bibliography, and selected observational measurements for several million astronomical objects (Wenger et al., 2000). It is maintained by the Centre de données astronomiques de Strasbourg (CDS), France. SIMBAD was created by merging the Catalog of Stellar Identifications (CSI) and the Bibliographic Star Index as they existed at the Meudon Computer Centre until 1979, and then expanded by additional source data from other catalogues and the academic literature. The first online interactive version, known as Version 2, was made available in 1981. Version 3, developed in the C language and running on UNIX stations at the Strasbourg Observatory, was released in 1990. Fall of 2006 saw the release of Version 4 of the database, now stored in PostgreSQL, and the supporting software, now written entirely in Java. Simbad is prepared to deliver resource profiles and to format the query outputs in a standard way, for instance XML (Ochsenbein et al., 2000). The main access point to Simbad is the WWW home page<sup>3</sup>; there is a mirror copy at SAO, Harvard<sup>4</sup>. The object type refers to a hierarchical classification of the objects in Simbad, derived by the CDS team on the basis of the catalogue identifiers (as proposed by Ochsenbein & Dubois (1992)). As of 30 May 2016, SIMBAD contains information for 8,275,526 objects under 23,139,386 different names, with 318,536 bibliographical references and 13,873,639 bibliographic citations.

### **2.1.5. WEBDA**

WEBDA<sup>1, 5</sup> is a devoted database of open star clusters. It includes astrometric data in the form of coordinates, rectangular positions, proper motions, photometric measurements, and spectroscopic data, such as spectral classification, radial velocities, and rotational velocities (Zejda et al., 2012). In addition, it contains miscellaneous types of other data such as membership probabilities, orbital elements of spectroscopic binaries, and periods of variability for different kinds of variable stars, including a whole set of bibliographic references (Zejda et al., 2012). This said database provides information about 1100 open clusters in our Galaxy and in the Small Magellanic Cloud.

---

<sup>3</sup> <http://simbad.u-strasbg.fr/Simbad/>

<sup>4</sup> <http://simbad.harvard.edu/Simbad/>

<sup>5</sup> <http://webda.physics.muni.cz> (Mermilliod & Paunzen, 2003)

### **2.1.6. Aladin and SKYCAT**

Aladin is an interactive sky atlas allowing the user to visualize digitized astronomical images or full surveys, superimpose entries from astronomical catalogues or databases, and interactively access related data and information from the Simbad database, the VizieR service and other archives for all known astronomical objects in the field<sup>6</sup>. Aladin has been developed independently by the CDS since 1993 as a dedicated tool for identification of astronomical sources a tool that can fully benefit from the whole environment of CDS databases and services, and that is designed in view of being released as a multi-purpose service to the general astronomical community (Bonnarel et al., 2000). It is intended to become a major cross-identification tool, since it allows recognition of astronomical sources on the images at optical wavelength, and at other wavelengths through the catalogue data (Bonnarel et al., 2000). Expected usage are searching for counterparts of sources detected at various wavelengths, and applications related to careful identification of astronomical objects, supply to needed catalogues for the CDS and database quality control (Bonnarel et al., 2000). The SKYCAT tool is developed at ESO (Albrecht et al., 1997) addressed this concern in the context of the European Southern Observatory scientific environment.

### **2.1.7. Online Digitized Sky Surveys**

The Online Digitized Sky Surveys server at the ESO Archive provides access to the DSS1 and DSS2 surveys produced at the Space Telescope Science Institute through its Guide Star Survey group. The images of these surveys are based on photographic data obtained using the Oschin Schmidt Telescope on Palomar Mountain and the UK Schmidt Telescope. The plates were processed into the present compressed digital form with the permission of these institutions. See the copyright notices. Other versions of DSS are available from the STScI - DSS form and the CADC - DSS form. The entire DSS1 and DSS2 data are stored on magnetic disks. Retrieval time takes less than 5 seconds for any field less than 20 arcmin in size<sup>7</sup>.

## **2.2. Astronomical Catalogue**

Jaschek (1989) defined a catalogue as a long list of ordered data of a specific kind, collected for a particular purpose. Moreover, catalogues are summarized the information/results of astronomical surveys. The said astronomical surveys are the main source for discovery of astronomical objects and accumulation of observational data for further analysis, interpretation, and achieving scientific results. The important catalogues of the cluster and stellar astronomy is discussed as below,

### **2.2.1. PPMXL catalogue**

The PPMXL catalog combines the USNO-B1.0 database of Monet et al. (2003) (data referred as first epoch images) and the 2MASS database of Skrutskie et al. (2006) (data referred as second epoch images) yielding the largest collection of proper motions in the International Celestial Reference Frame (ICRF) to date (Roßer et al., 2010). Further, it has contained the mean positions and proper motions of all objects of brightest magnitudes down to V20 mag (total 910 million objects, in which 410 million objects have photometric data from 2MASS catalog). The mean errors in the estimation of proper motions vary from 4 mas/yr (milli-arcseconds per year) for  $J < 10$  mag to more than 10 mas/yr at  $J > 16$  mag (Khalaj & Baumgardt, 2013). Roßer et al. (2010) have pointed out that the magnitude and color dependent systematic errors in the PPMXL catalog are difficult to be determined due to no independent reference on ICRS at fainter magnitude (Wu, Zhen-Yu et al., 2011). The 2MASS observations were conducted using two dedicated 1.3 m diameter telescopes located at Mount Hopkins, Arizona, and Cerro Tololo, Chile.  $256 \times 256$  NICMOS3 (HgCdTe) arrays manufactured by Rockwell International Science Center (now Rockwell Scientific), were used which give field-of-view of  $8.5 \times 8.5$  and pixel scale of 2 pixel<sup>-1</sup> (Tadross, 2011). Each telescope is equipped with a three-channel camera. Each camera consists of a liquid nitrogen cryostat which contains three NICMOS3 arrays. During the observations each array views the same region of the sky. NIR 2MASS photometry provides J (1.25 $\mu$ m), H (1.65 $\mu$ m), and Ks (2.17 $\mu$ m) band photometry of millions of galaxies and nearly a half-billion stars Carpenter (2001). This survey has proven to be a powerful tool in the analysis of the structure and stellar content of open clusters Bonatto & Bica (2003). 2MASS Survey observations did not enable a direct measurement of the absolute calibration of the 2MASS photometric system. Cohen et al. (2003) have determined photon counting relative spectral response curves (RSRs) for the 2MASS system by combining the transmission and QE curves.

The QE based component was converted to yield photon-counting RSRs by multiplying by wavelength and renormalized (Bessel, 2000). The gain of the 2MASS electronic is approximately 8 electrons per analog-to-digital count and read out noise is 40 electrons. The 2MASS data base provides photometry in the near infrared J, H and Ks bands to a limiting magnitude of 15.8, 15.1 and 14.3 respectively, with a signal to noise ratio (S/N) greater than 10.

---

<sup>6</sup> <http://aladin.u-strasbg.fr/>

<sup>7</sup> <http://archive.eso.org/dss/dss/>

### 2.2.2. Wise catalogue

The Wide-field Infrared Survey Explorer (WISE; Wright et al. 2010) in themid-IR is a NASAMedium Class Explorer mission that conducted a digital imaging survey of the entire sky in the 3.4 $\mu$ m (W1), 4.6 $\mu$ m (W2), 12 $\mu$ m (W3) and 22 $\mu$ m (W4) bands. Moreover, the angular resolutions of these bands are 6.1", 6.4", 6.5" and 12.0" respectively. In addition, WISE has produced and released a reliable Source Catalog containing accurate photometry and astrometry of over 300 million objects. All four bands were imaged simultaneously during each exposure, and the exposure times were 7.7 sec in W1 and W2 and 8.8 sec in W3 and W4. All of the individual exposures that met minimum requirements for image quality and noise levels were combined to form the All-Sky Release Image Atlas and Source Catalogue. The WISE Source Catalog contains the attributes for 563,921,584 point-like and resolved objects detected on the Atlas Intensity images.

### 2.2.3. UCAC4

UCAC4 (Zacharias et al., 2013) is an all-sky star catalogue covering mainly 8 to 16 mag stars in a single passband between V and R. Furthermore, the positional errors are about 15 to 20 mas for stars in the 10 to 14 mag range. The proper motion in this catalogue have been derived for around 113 million stars utilizing about 140 other star catalogues (including old SPM catalogue, Hipparcos and Tycho) with significant epoch difference to the UCAC4 CCD observations.

### 2.3. The Filters

Above prescribed databases are having stellar magnitudes in the different part of radiation. These said magnitudes are showing the strength of emitted radiation through the stellar activities. Moreover, these stellar magnitudes are provides the extrinsic colours of the stars, which are provide the crucial information of electromagnetic (em) radiation. The said information is useful to constrain the associated dynamical and evolutionary phenomenon of the interested target. Such radiation based information can be obtained through the filters or passbands. Thus, the function of filters is sensitiveness towards to incident radiation. Moreover, it seems that paasbands are sensitive for the limited spectral range of a star light. These filters is also reduce the overall intensity of the stellar light due to the reflection of outside radiation of the fixed wavelength range of filters.

Table 1: Details of various filter systems.

Filter	$\lambda_{eff}$ Å	Band-width Å	Glass combination of filter (thickness in mm)
U	3650	680	UG 1(2) + CuSO4 Solution(5)
B	4400	980	GG 385(2) + BG 18(1) + BG 12(1) + KG 3(2)
V	5500	890	GG 495(2) + BG 12(2) + KG 3(2)
R	6500	2200	OG 570(2) + KG 3(3)
I	8000	2400	RG 9(3) + WG 305(2)
J	12350 $\pm$ 60	1620 $\pm$ 10	
H	16620 $\pm$ 90	2510 $\pm$ 20	
K	21590 $\pm$ 110	2620 $\pm$ 20	
W1	34000	6625 $\pm$ 12	
W2	46000	10423 $\pm$ 11	
W3	120000	55069 $\pm$ 169	
W4	220000	41013 $\pm$ 448	

Several filters are used in the optical and infrared photometry. Johnson UBV and Cousins RI filters are used in the optical photometry. Similarly, the near-infrared (NIR) data has been gathered in the JHK photometric band. The summarized details of various filters are listed in Table 1. The well defined set of passbands is defined as the photometric system. The filters are made by the combination of colored glasses of WG, GG (Sulpher and Cadmium sulfide) and OG (Cadmium selenide). The UG (violet) and BG (blue) are made of ionic glasses.

### III. Data Reduction of Optical Photometry

The raw images of targets are directly gathered by the CCD camera of the telescopes. These images are highly influenced and degraded by the turbulence of atmosphere conditions, telescope motion, poor focusing, geometric distortion due to optical system, target position, presence of charge diffusion in the detector and electronics of the CCD. Moreover, the CCD images is also affected by superimpose of various intrinsic /extrinsic noises. As a result, the reduction processes of these images are needed to extract the information about the position, luminosity and image shape of detected objects in the CCD frame. These image-processing



procedures help to us for compensating deformation and restoring the original geometry. This data reduction is carried out through the various mathematical operations (addition, subtraction, multiplication or division of a frame by another frame) and numerous other manipulations like logarithms, statistics, smoothing, contouring and magnitude calculations etc. The data reduction is carried out by various image processing softwares such as IRAF<sup>8</sup>, MIDAS<sup>9</sup>, DAOPHOT<sup>10</sup> etc. Generally, the prescribed image processing is divided into three basic stages such as: (i) Pre-processing, (ii) processing and (iii) post processing.

### 3.1. Pre-processing

The transformation of the raw images into the science images known as the pre-processing of the photometry. In the pre-processing, the raw images are defined as the digital transformation of the interested sky patch. The raw images are group of the bias frames, flat frames and raw object frames. The bias subtraction, flat fielding, cosmic ray reduction and aligning are the major steps of the pre-processing. The bias and flat frames must be collected for the same observational night of the target object. The detail description of these steps are given as below,

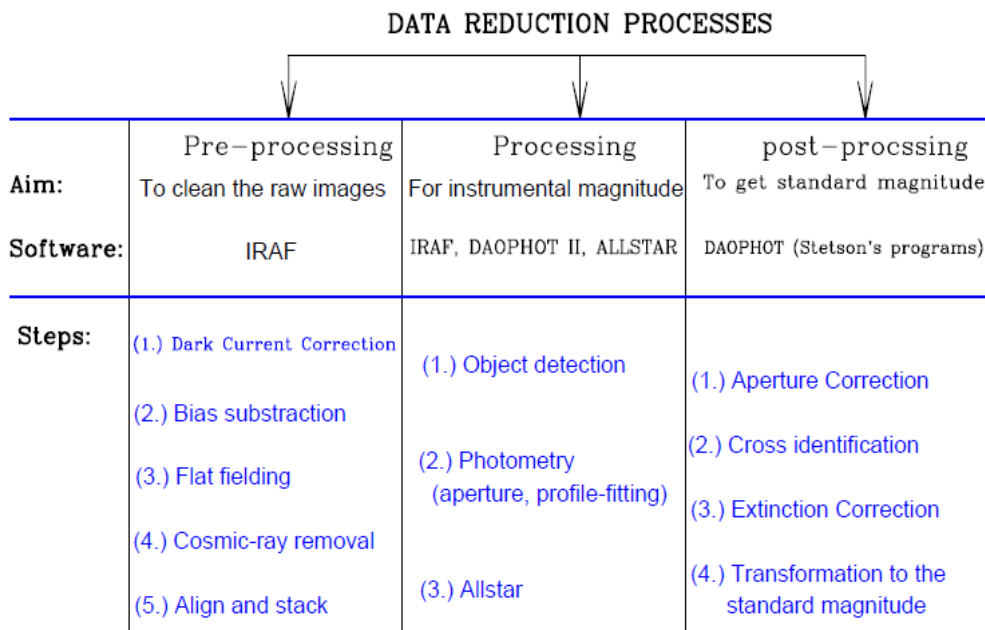


**Figure 1:** The Systematic chart of reduction processes of the astronomical data.

#### 3.1.1. Bias subtraction

Bias frames are those frames, which are taken with zero exposure time, which provides the information of readout of CCD at the case of closed shutter. The bias value in a CCD image is usually a low spatial frequency variation throughout the array, caused by the CCD on-chip amplifiers. Furthermore, there are also some negative signals in the pixels of CCD, which cannot be converted into counts. As a result, some positive electronic offset is needed to a CCD to overcome from this situation. Moreover, the bias frame allows to us to determine the underlying level within each object frame. A bias frame contains both the DC offset level and the variations on that level. In principal, this label is constant both in time and space across the pixels of CCD. As a result, number of bias frames was acquired at regular intervals. The bias subtraction is the first step of the photometric processing to remove the DC voltage from the images. Since, the variation of level is found in the statistical fashion, therefore a median bias image of more bias frames (5 to 10) were taken (Gilliland, 1992). This median bias frame is subtracted from the raw object frames and flat frames. ZEROCOMBINE task in IRAF is used to obtain a median bias frame.

<sup>8</sup> IRAF stands for Image Reduction and Analysis Facility distributed by the National Optical Astronomy Observatories which is operated by the Association of Universities for research in Astronomy, Inc. under cooperative agreement with the National Science Foundation

<sup>9</sup> MIDAS stands for Munich Image and Data Analysis System designed and developed by the European Southern Observatory ESO in Munich, Germany

<sup>10</sup> DAOPHOT stands for Dominion Astrophysical Observatory Photometry

### **3.1.2. Flat fielding**

The response of all pixels of CCD does not same, whereas they represent same sensitivity. As a result, spatial noise is added in the CCD frames due to the different react of adjacent pixels for the identical. Since, sensitivity variation of the pixels occurs 10 to 20% of the mean sensitivity, therefore correction of non-uniform sensitivity of pixels is carry out through an image of uniform background [either on sky or flat field screen on the inside of dome (Massey & Jacoby, 1992)]. Moreover, such type frames are known as the flat frames. These frames of good sky region for twilight flats has been determined to be an area 13 east of zenith just after sunset (Chromey & Hasselbacher, 1996). To achieve large-scale and uniform flat fields, an isotropic diffuser is placed in front of the telescope and illuminated by reflected light from the dome screen Zhou et al. (2004). These frames are needed for each wavelength region and different instrumental setup used for which object frames are taken. If  $I(x,y)$  and  $F(x,y)$  are the bias subtracted raw object and flat images then the processed image is represented as  $E(x,y) = K(I(x,y)/F(x,y))$  where  $K$  is the multiplier coefficient (Buil, 1991). The value of  $K$  is approximately to the average intensity of the flat field and it is used to find the initial level of the processed image. The median frame of 5 or more bias subtracted flat frames is used to image calibration (Massey & Jacoby, 1992; Tobin, 1993) due to the statistical fluctuation behaviour of the flat images. The said median flat frame is produced by the "FLATCOMBINE" task of the IRAF package. We are utilized to CCDPROC task of the IRAF for getting the cleaned object frame, which is free from CCD noise and non-uniform pixel variations.

### **3.1.3. Dark current correction**

Since, CCD is a electronic detector, therefore some associated charge is also generate due to the thermal fluctuation. This charge is calculated through the registered dark counts and these said dark counts are generated for the same exposure time of objects with closed shutter. It is believed that Since, this thermal dark current is very rapidly decaying with the decreasing temperature, therefore negligible dark current is obtained by cooling the CCD to a temperature somewhere between those of dry-ice and liquid Nitrogen. In the 1.04 case of Sampurnanand telescope (Manora peak, Nainital), the CCD cool by a liquid nitrogen to  $-120^{\circ}\text{C}$ , therefore the dark correction is not applied for gathered data through it due to very low dark current production for 30 min long exposure with above prescribed temperature.

### **3.1.4. Removal of cosmic rays**

There are several bright specks with one or two pixel size, which are randomly appeared in the captured images of the objects. These bright specks are appeared due the cosmic rays and their stellar profile is different compared to the real stellar objects. Moreover, this dissimilarity of cosmic rays is used to separate them from the stars of object frames. These said cosmic rays are not always cosmic but also arise by weakly radioactive materials used in the construction of CCD dewars Florentin-Nielsen et al. (1995). The "COSMICRAYS" task of the IRAF software is used for the removal of cosmic rays from a cleaned object frame.

### **3.1.5. Aligning and stacking process of the frames**

It is needed to adding counts of interest fainter objects for acquiring stellar information. For this purpose, the programmed image frames are combined after align, which leads increased signal to noise ratio. If the time series data is captured for the interest objects then the pixel coordinates of the stars are varied frame to frame and night to night, which also shows need of align processes of images. This said processes are carry out for 6 those images, which are captured for same filter. The "IMALIGN" or "GEOMAP and GEOTRAN" tasks of IRAF package are utilized to align the images. These aligned images are stacked through the "IMCOMBINE" task of IRAF software. To align the images, first a reference frame is to be selected, displayed and finds out the pixel co-ordinates of stars through the "CENTER" task of IRAF package. About 10 points (coordinates of stars) spread over entire CCD frame should be taken. These co-ordinates are listed in a file which is automatically created by the center task. Now after displaying another image which is to be aligned, the pixel co-ordinates of the same stars are find out. The difference (shift in position) between co-ordinates of reference image and image to be aligned is calculated and noted in a specific file. Such files of each image are used in the "IMALIGN" task of IRAF package to align the images w.r.t. the reference image.

## **3.2. Processing**

After getting cleaned image from the pre-processing, the second stage is extraction of stellar positions and magnitudes from a given CCD image. The photometry is the main step of processing and this is performed by using the DAOPHOT II<sup>11</sup> (Stetson, 1987, 1992). The different steps of the photometry are as follow,

---

<sup>11</sup> It is the revised version of Dominion Astrophysical Observatory Photometry software.



### **3.2.1. The detection of stellar objects**

The detection of objects is needed to proceed the photometry by rejecting bad pixels, rows and columns etc. The “FIND” routine is an automatic detection algorithm of DAOPHOT package and used to stellar detection within the CCD images. Moreover, this routine also differentiates between stars, cosmic rays and galaxies. For this purpose, this routine is performed following tasks,

1. Detects and locates small, positive brightness enhancement within an image.
2. Distinguishes stellar images from random noise peaks in the data, images of galaxies or other extended objects and cosmic rays or any high energy particles.
3. Recognizes when a seemingly extended object consists of two or more overlapping stellar images.

FIND routine convolves the image to locate a star in a pixel by fitting an analytic Gaussian profile (whose full width at half maximum (FWHM) is equal to the FWHM of the objects as given by us) to the brightness values of surrounding sub-array of pixels. It tries to locate stars by going through pixel by pixel and looking for locations where the Gaussian profile fit is good i.e where the central height of the best fitting model Gaussian profile achieves a large, positive value probably lies near the centre of star image. In this way FIND identifies the X and Y position of stars in the frame and catalogues them in a file.

### **3.2.2. Photometry**

The exact meaning of the photometry is photon meter, which provides quantitative (numerical) values for the brightness of objects in the frame. There are two techniques for measuring the intensity/instrumental magnitudes; aperture photometry and point-spread-function (PSF) photometry. Both methods are discussed as below,

#### **Aperture photometry:-**

It gives an opportunity to measure the brightness of an object without including possible contributions from contamination sources such as sky, pixel defects or other stars and galaxies. If a CCD frame contains few stars, then the simulate photometry is carried out by simply defining a circular geometric region. This region is defined as an “aperture”. Thus, aperture photometry does not depend on the actual shape of the source PSF but simply collects and sums up the observed counts within a specified aperture centered on the source (Howell, 2006). We estimates sum up the photons detected within an aperture centered around a star and also finds sum up the sky photons detected within a star free region of the same area elsewhere in the frame. The difference of these two sums is computed in this photometry. The resulting counts corresponding to a particular star are converted into magnitude scale. The “PHOT” routine of DAOPHOT II and IRAF packages is used for this purpose. The routine allows specifying a series of 4 to 12 increasing concentric apertures and an annulus to evaluate the sky. This method is for the NASA Kepler Discovery mission to search for terrestrial size extra-solar planets, the GAIA Mission, and numerous ground-based time-resolved photometric surveys even in fairly crowded fields (Howell et al., 2005; Tonry et al., 2005). Larger aperture adds sky noise and may introduce systematic errors due to the noise in the sky level. The usual approach to minimise these problems is to examine the curve-of-growth. The said aperture photometry performs well for isolated bright stars but it does not work for crowded and faint stars.

#### **Point spread function photometry:-**

The S/N of faint stars becomes poor and thus the estimated magnitude has large error. In case of crowded field region, other neighbour stars flux also may influence the aperture of any star. This condition creates limitation for estimating the magnitude of star through aperture technique. The point spread function (PSF) provides an opportunity to overcome above prescribed difficulties. Moreover, the PSF fitting may be the only method capable of producing scientifically valid results for the crowded fields such as star clusters (Stetson, 1987, 1992). Since the stars in given a frame are observed at same time and in identical observing conditions they would have the same profile and same form and differ from one another only in intensity by a scaling ratio. This property of the image is the basic principle of PSF fitting photometry. The stellar image is affected by the irregularities of the instrument (telescope observations, tracking errors, camera optics etc.) and the seeing in the ground based observations. In this background, the various approaches have been used to determine the stellar PSF of a given frame. The PSFs are the two- 7 dimensional (2-D) distribution produced in the detector by the images of astronomical point sources. The profile fitting method is based on modeling of such images of stars and then fitting to other stars of the frame. PSFs can be modeled by a number of mathematical functions, the most common tree function are given as below,

Gaussian

$$G(r, a) \propto e^{-\frac{r^2}{2a^2}},$$

Modified Lorentzian

$$L(r; a, b) \propto \frac{1}{1 + (1 + r^2/a^2)^b},$$

and Moffat

$$M(r; a, b) \propto \frac{1}{(1 + r^2/a^2)^b}$$

where  $r$  is the radius and  $a$  and  $b$  are fitting parameters (Stetson, 1989; Stetson et al., 1990). These types of functional forms can be used to define the PSF for a star within an image by the assumption that they provide a good representation of the data itself and the method is called analytical. This analytical method has the advantage of integrating numerically over the entire stellar image but the problem being that the function used to fit the profile can only be approximated. The other PSF method is known as empirical where it is possible to simply store the observed profile of several bright stars as a data array  $Q(i, j)$ . The empirical method has the advantage that it uses the observed profile, but the drawback in this case is that near the central region of the stellar image, the brightness varies too rapidly between the adjacent pixels to be interpolated correctly. Therefore, the better results can be obtained by combining above two methods (Stetson, 1987; Sagar, 1987).

The Gaussian PSF routine of DAOPHOT is used to determine the PSF of stars of images. In this routine, we first identified a few fairly isolated bright stars in the frame and determined the PSF iteratively by detecting and deleting the neighbors present inside the PSF radius. We repeated this procedure till we got the few isolated stars devoid of neighbors. In this routine an analytic function is fitted to the observed stellar profiles and residuals are stored in look-up table that contains the difference between mathematical model of the PSF and an observed PSF. Furthermore, the final PSF was determined through the above prescribed isolated stars. It is need to take utmost care in selecting such isolated stars because a star should not be used to define PSF if there is either a neighbor within one fitting radius or bad pixels within the profile of the star.

**3.2.3. Allstar routine** The resultant PSF by the above prescribed method was applied to all the stars with aperture photometry using the routine ALLSTAR. This technique uses deconvolution procedure for magnitude determination of overlapping stellar images. It is therefore effectively used accurate photometric work in star clusters. In order to verification of detection and measure of stars, the measured stars were subtracted from the frame by using the option of ALLSTAR. This option uses the PSF file and the above file obtained after PSF photometry and outputs an image display. If there were stars still left in the picture then we detected them manually and repeated the whole procedure of photometry till we got the clean residual image. The output of ALLSTAR gave us the ID numbers of detected stars, final  $x$  and  $y$  pixel positions of the stars, their magnitudes with errors, sharpness, roundness value and  $\chi$  value of PSF fitting. The estimated errors in the magnitude determination were used to reject the bad measurements. Moreover, this routine is also provides information about number of iterations before convergence for least-squares-fit, estimated modal sky value and differentiating parameter of star, galaxy, cosmic rays etc.

### 3.3. Post-processing

Some counts of the object are left out in the wings of the stellar profile in the PSF photometry due to fixed aperture, whereas a light growth curve of objects is constructed in the aperture photometry and this light (flux) is defined as the function of the radius. The flat growth curve leads to be estimation of total instrumental magnitude of stars. To compare the results from different telescopes and instrument systems, under different observing conditions, we need to bring them into standard magnitude systems. On this background, the computation of standard magnitude is carried out by the various corrections, which shows need of calibration of instrumental magnitudes (e.g. DaCosta 1992; Palmer and Davenhall 1999 for general discussions). These corrections will be provided a list of stars with known positions and their apparent instrumental magnitudes relative to an arbitrary zero point. The essential steps of estimation of standard magnitude is given as below,

#### 3.3.1. Aperture-correction

Aperture photometry is applied for the several selected, bright, unsaturated, isolated stars of each CCD image using a series of apertures of increasing size. Moreover, these selected stars are well-behaved to ensure a good determination of the total instrumental magnitude. In profile fitting photometry, the instrumental magnitude of a star comes from the height of a model PSF. For this purpose, frame is scaled to the recorded intensity values inside the stars image. The above prescribed magnitude is limited according to the chosen aperture which is also applicable to correct the counts left out in the wings of the stellar profile. This said correction are carried out by

the process of determining the aperture growth curve and is known as the aperture correction. The prescribed correction is applied to the PSF magnitudes for getting the aperture instrumental magnitudes, which is carried out by the DAOGROW routine (see Stetson 1990 for details). In the alternative way, first of all, we had to take a subset of stars. Moreover, the average difference value has been computed for five/six stars. The said difference value is found between the instrumental magnitude and total instrumental magnitude. This average difference is used to convert the other instrumental magnitudes into total instrumental magnitudes of the stars. This prescribed procedure of aperture correction is carried out for each filter separately.

### 3.3.2. Cross identification

The process of cross identification of stars is necessary for determining the standard magnitudes and colours. The positions are slightly changed in frame of different filter and different epoch of a particular telescope whereas the pixel coordinates are entirely distinguish for the various frames of various telescopes. This said process is carried out through the DAOMATCH programme of DAOPHOT II. In this programme, stars are recognized in the form of triangles due to fact that these said triangles are not changed their shape according to the change of positions, orientations and sizes. Moreover, these triangles are translated, rotated and scaled but clearly identified by the DAOMATCH programme. In this connection, the bright stars are chosen first due to their most detectable property. The said programme is established the coordinate transformation equations through the common 30 bright stars between the various frames with respect to a reference frame. Since, some bright stars do not identify in each frame of target field, therefore, DAOMASTER programme is applicable to identify the stars. This programme depends on the approximate transformation equation provided by DAOMATCH. In addition, this programme reads in all the star lists for that field and cross-matches all stars by spatial proximity. if after transformation to the coordinate system of the master frame, a star lies within the specified distance of a star in the master list, it is provisionally identified with that star; if it lies near no star in the master list it is added to the list as a possible new detection.

### 3.3.3. Atmospheric extinction correction

The light of celestial objects is reduced due to the its absorption and diffusion by the medium, these said phenomena occur due to the propagation of the terrestrial atmosphere. These effects are found to be minimum at the zenith whereas maximum at the horizon. The path length through the atmosphere is known as air mass (X). It is approximately the secant of the zenith distance, but rises more slowly as the star approaches the horizon, becoming 1% less than the secant at 17 altitudes. The said air-mass is computed through the equation (Hardie, 1962),

$$X = \sec Z - 0.0018167(\sec Z - 1) - 0.002875(\sec Z - 1)^2 - 0.0008083(\sec Z - 1)^3 \text{ where, } \sec Z = (\sin \phi \sin \delta + \cos \phi \cos \delta \cosh)^{-1}.$$

Moreover,  $\phi$ ,  $\delta$  and  $h$  are the observer's latitude, the declination and the instantaneous hour angle of the star respectively. The air mass is defined as the thickness of the atmosphere crossed by the light rays. In this connection, the air mass is considered to be 1 at the zenith, approximately 2 at an altitude of 600 and its value rises to larger values with increasing Z. From the plots of  $v$ ,  $(b-v)$ ,  $(u-b)$ ,  $(v-r)$ ,  $(r-i)$  and  $(v-i)$  against air mass for the comparison stars on each night, the atmospheric extinction coefficients  $k_v$ ,  $k_{(b-v)}$ ,  $k_{(u-b)}$ ,  $k_{(v-r)}$ ,  $k_{(r-i)}$  and  $k_{(v-i)}$  were determined using the method of linear least squares. This atmospheric extinction is defined as the loss of starlight in passing through the Earth's atmosphere. Most of the loss arises from Rayleigh scattering by molecules of nitrogen and oxygen. At certain wavelengths there is absorption from molecules of oxygen, ozone, and water vapour. Atmospheric extinction is proportional to the airmass and the atmospheric pressure. At sea level and in a perfectly clear sky a star 800 from the zenith appears 1 mag. fainter than it would at the zenith. This in turn is 0.3 mag. fainter than if no atmosphere were present. After applying the extinction corrections to the observed quantities  $v$ ,  $(b-v)$ ,  $(u-b)$ ,  $(v-r)$ ,  $(r-i)$  and  $(v-i)$  we obtained the values of instrumental magnitudes and colours as seen outside the atmosphere (denoted by zero subscripts) for comparison and programme stars using the relations:

$$\begin{aligned} v_0 &= v - k_v X, \\ (b - v)_0 &= (b - v) - k_{(b-v)} X, \\ (u - b)_0 &= (u - b) - k_{(u-b)} X, \\ (v - r)_0 &= (v - r) - k_{(v-r)} X, \\ (r - i)_0 &= (r - i) - k_{(r-i)} X, \\ (v - i)_0 &= (v - i) - k_{(v-i)} X. \end{aligned}$$

### 3.3.4. Standardization

The instrumental magnitudes are converted into standard magnitudes through the following transformation equations,

$$u_{CCD} = U + a_0 + a_1(U - B) + a_2X$$

$$b_{CCD} = B + b_0 + b_1(B - V) + b_2X$$

$$v_{CCD} = V + c_0 + c_1(B - V) + c_2X$$

$$r_{CCD} = R + d_0 + d_1(V - R) + d_2X$$

$$i_{CCD} = I + e_0 + e_1(V - I) + e_2X$$

$a_0, b_0, c_0, d_0$  and  $e_0$  are the zero points;  $a_1, b_1, c_1, d_1$  and  $e_1$  are the colour coefficient;  $a_2, b_2, c_2, d_2$  and  $e_2$  are the earth's atmospheric extinction coefficients and  $X$  is the air mass.  $U, B, V, R$  and  $I$  are the standard magnitudes, whereas  $u_{CCD}, b_{CCD}, v_{CCD}, r_{CCD}$  and  $i_{CCD}$  are the aperture instrumental magnitudes. For this purpose, the second order colour corrections are ignored due to their least values compare to the other errors of photometric data reduction procedure. In various work, the above prescribed calibration is carried out through the observation of standard star fields of Landolt (1992) and Persson et al. (1998).

## IV. The general astronomical routines

### 4.1. Magnitude of objects

The stellar magnitude of a stellar object is computed through the following formula (Howell, 2006),

$$\text{Magnitude} = -2.5\log(I) + C, \quad (1)$$

where  $I$  is the source intensity per unit time (flux), and  $C$  is an appropriate constant (usually 23.5-26 according to observing sites). This flux is computed as below (Merline & Howell, 1995),

$$I = S - n_{pix} - \bar{B},$$

where  $S$  shows contribution of source of area  $A$  with background sources  $n_{pix} - \bar{B}$  within  $A$  and  $\bar{B}$  is the mean background contribution of each pixel. If, two stars are seems to be one by naked eye, then their combined magnitude is defined as follow,

$$m = m_1 - 2.5\log[1 + \text{antilog} - 0.4(m_2 - m_1)]$$

where  $m_1$  and  $m_2$  are their individual magnitudes. For example, the combined magnitude of two stars each of magnitude 1 is 0.25.

#### 4.1.1. Colour-excess

The colour-excess is the difference between the observed colour of a star and its intrinsic colour index due to interstellar absorption. Interstellar absorption decreases towards longer wavelengths, so its effect is always to make a star appear redder; colour excesses are therefore always positive. The symbol for the colour excess in  $B - V$  is  $E(B - V)$ , and similarly for other colours.

#### 4.1.2. colour index

The difference between the apparent magnitudes of a star at two different wavelengths, as measured through filters of different colours, e.g.  $B$  (blue) and  $V$  (yellow-green).  $B - V$  and  $U - B$  are typical colour indices. In Johnson photometry and \*Kron- Cousins  $RI$  photometry, all colour indices are made zero for a star of spectral classification AOV (e.g. Vega). Generally, hotter stars have negative colour indices, and cooler stars positive ones. Nowadays, colour index is usually shortened to 'colour'.

#### 4.1.3. Colour-magnitude relation

The correlation between colour index and absolute magnitude of stars on the lower main sequence is also known as colour-luminosity relation. If the absolute magnitudes of stars intrinsically fainter than the Sun are plotted against colour index, there appears a tight relationship which defines the \*main sequence. The slope of the relationship depends on the colour index used. If  $(B - V)$  is used for the colour then the relationship is much shallower than for  $(V - I)$ .

#### 4.2. Hertzsprung-Russell diagram (HR diagram)

A graph on which a measure of the brightness of stars (usually their absolute magnitude) is plotted against a measure of their temperature (either spectral type or colour index). The diagram shows how the luminosities and surface temperatures of stars are linked. From a star's position on the diagram, astronomers can estimate its mass and the stage of its evolution. Most stars lie on the main sequence, a strip which runs from the upper left to the lower right of the diagram. A star on the main sequence is burning hydrogen in its core, and during this phase of its life will remain at a point on the diagram that is determined by its mass. Other areas of the HR diagram are populated by stars that are not burning hydrogen in their cores, but may be burning hydrogen in a thin shell. The most prominent of these areas is the giant branch, consisting of stars which have exhausted the hydrogen fuel in their cores.

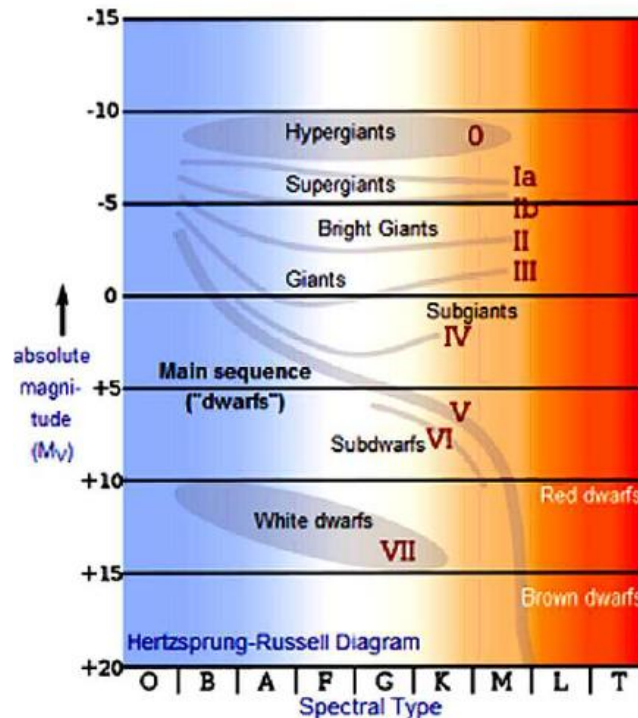


Figure 2: The various stellar groups in the HR diagram.

##### 4.2.1. Asymptotic giant branch star (AGB star)

A star that occupies a strip in the Hertzsprung-Russell diagram that is almost parallel to, and just above, the giant branch. Stars evolve from the horizontal branch to the asymptotic giant branch when they have exhausted the helium in their core and are burning it in a shell.

##### 4.2.2. Giant branch

The Giant branch region of the Hertzsprung-Russell diagram extends diagonally to the upper right of the main sequence, containing giant stars. The giant branch ranges from stars with a surface temperature similar to the Sun's, but luminosity some 30 times greater, to cooler but even more luminous stars. Giants greater than about 1 solar mass are separated from the main sequence by the Hertzsprung gap.

##### 4.2.3. Sub-giant branch

A star of Sub-giant branch has exhausted the hydrogen at its centre and is evolving into a giant. They are of luminosity class IV. The sub-giants we see are usually less massive than the Sun, because more massive stars move very quickly through this stage into giants. Low-mass stars take many billions of years to evolve this far, so low-mass sub-giants are very old. A sub-giant branch on the HR diagram, linking the main sequence to the giant branch, is therefore found only for old clusters such as globular clusters.

##### 4.2.4. Horizontal branch

A horizontal strip of stars in the Hertzsprung-Russell diagram of globular clusters, comprising stars somewhat bluer and fainter than those on the giant branch. These stars are thought to be burning helium in their core and hydrogen in a surrounding shell. They are of 0.6-0.8 solar masses, of which more than half is in the helium-burning core, and have probably lost substantial mass through stellar winds during their giant phase. Stars typically spend 50-100 million years on the horizontal branch.

#### **4.2.5. Hertzsprung gap**

This gap is an area of the HR diagram containing no stars, between the top end of the main sequence (where stars are more massive than the Sun) and the \*giant branch. Stars cross this region very quickly once they leave the main sequence because their outer layers are expanding rapidly. While the star's luminosity remains roughly constant, the surface temperature goes down so that the star follows an approximately horizontal path from left to right on the HR diagram.

#### **4.2.6. Henyey track**

The roughly horizontal path on the Hertzsprung-Russell diagram followed by a pre-main- sequence star with mass greater than about 0.4 solar masses. The track takes it on to the main sequence after it has descended the Hayashi track. Stars on Henyey tracks are becoming hotter, and therefore bluer, as they contract. The contraction ends once the core is hot enough for hydrogen burning to begin and the star joins the main sequence. Whereas stars on Hayashi tracks are fully convective, those on Henyey tracks are radiative.

#### **4.2.7. Hayashi track**

The nearly vertical path on the Hertzsprung-Russell diagram that is followed by a fully convective star as it evolves. Forming stars (proto-stars) descend such tracks on to the main sequence, becoming less luminous with time but maintaining a roughly constant surface temperature. The process occurs in reverse in old stars leaving the main sequence for the giant branch.

#### **4.2.8. Sub-dwarf**

A star of this category lies appreciably below the main sequence on the Hertzsprung-Russell diagram, and is bluer than a main-sequence star of the same luminosity. Sub-dwarfs belong to Population II, being stars from the galactic halo which are passing through the solar neighbourhood. They differ from normal dwarfs in having a low abundance of heavy elements.

#### **4.2.9. Super-giants**

These are the largest and brightest type of stars, with a luminosity of about 10 000 100 000 times the Sun's, and a diameter from 20 to several hundred times the Sun's. Stars of at least 10 solar masses become supergiants when they swell up and leave the main sequence towards the end of their lives. They occupy a band at the top of the Hertzsprung-Russell diagram and are of luminosity class I.

#### **4.2.10. zero-age horizontal branch**

That part of the Hertzsprung-Russell diagram occupied by low-mass stars that have just undergone the helium flash. The scatter in properties of stars on the zero-age horizontal branch is due to the range of stellar masses resulting from mass loss on the giant branch.

#### **4.2.11. zero-age main sequence (ZAMS)**

The ZAMS is a diagonal strip on the HR diagram occupied by stars that have just begun to convert hydrogen to helium in their cores. As this conversion proceeds, stars become slightly redder and more luminous, so they move upwards and to the right on the HR diagram. As a result, the main sequence is a broad band that is displaced slightly from this zero-age strip.

### **4.3. Astrometry**

The astrometry shows the measurement of positions, parallaxes, and proper motions on the sky. It can be divided broadly into two categories: global and small-field astrometry. Global astrometry is concerned with mapping and cataloguing positions and motions over large areas of sky. It was traditionally based on optical observations made with meridian instruments and astrolabes. The accuracy of all ground-based optical astrometry is limited by thermal and mechanical instabilities in the telescopes, but also mainly by uncertainties in the amount of atmospheric refraction. In small-field astrometry, relative positions are measured within the area observable with long-focus telescopes, by means of CCDs. The transformation of the pixel coordinates into the celestial coordinates is carried out by using online skycat software. In this routine, the frames of the digitized sky ESO catalogue are taken to be an absolute astrometric reference frame. A linear astrometric solution has been derived for the reference frame by using a data set of common stars between the coordinate of reference frame and USNOA2.0/2MASS catalogue. The said data set contain 4 columns as following: first and second columns are contained pixel coordinates (X,Y) from the reference frame, whereas third and fourth columns are contained the celestial coordinates ( $\alpha$ ,  $\delta$ ) of the cross-matched and well isolated bright stars. The ccmmap and cctran tasks of IRAF software package were used to derived a transformation equation for converting



(X,Y) into ( $\alpha, \delta$ ). In the case of best conversion of above prescribed coordinates, The RMS scattering of both right-ascension (RA) and declination (DEC) should be 0.1 arcsec.

#### 4.4. Calculation of stellar distance in the terms of arcmin

Since, the arcmin unit of RA and DEC directions are not same due to the spherical property of sky, therefore, the distances of  $i^{\text{th}}$  star from cluster's center have estimated in RA and DEC directions ( $ra_i$  and  $dec_i$  in same radians unit) respectively. The following transformations equations have been used for this purpose:

$$\begin{aligned} ra_i &= \sin(r_i - r_c) \times \cos(d_c) \\ dec_i &= \sin(d_i - d_c) \times \cos(r_i - r_c) \end{aligned} \quad (2)$$

where  $r_i$  and  $d_i$  are the RA and DEC values of  $i^{\text{th}}$  stars in radians while the  $r_c$  and  $d_c$  are the the center coordinate of cluster in the unit of radians. These radian values have been transformed in absolute arcmin values by following relation:

$$\begin{aligned} RA_i &= ra_i \times \frac{10800}{\pi} \\ DEC_i &= dec_i \times \frac{10800}{\pi} \end{aligned}$$

Thus, the radial distance of  $i^{\text{th}}$  star from cluster center has been estimated as

$$D_i = \sqrt{RA_i^2 + DEC_i^2} \quad (4)$$

#### 4.5. Galactocentric coordinates and distance

The elliptic coordinate ( $\alpha, \delta$ ) are converting into galactic coordinate ( $l, b$ ) through the following transformation equations,

$$\begin{aligned} b &= \sin^{-1} [\cos\delta \cos 27.4 \cos(\alpha - 192.25) + \sin\delta \sin 27.4] \\ l &= \tan^{-1} \left( \frac{\sin\delta - \sin b \sin 27.4}{\cos\delta \cos 27.4 \sin(\alpha - 192.25)} \right) + 33, \end{aligned}$$

where (192.25, 27.4) ( $\alpha_{galactic}, \delta_{galactic}$ ) is the center coordinate of our galaxy and  $l=33$  represents the ascending node of the galactic plane. The galactic center of interested object is defined as ( $\alpha, \delta$ ) and the heliocentric distance of the interested object is denoted by  $R_{Ob}$ . The galactic coordinate of interested object is estimated by following relations:  $X = R_{Ob} \cos l \cos b$ ,  $Y = R_{Ob} \sin l \cos b$  and  $Z = R_{Ob} \sin b$ . Furthermore, the Galactocentric distance ( $R_{GO}$ ) is estimated by a relation as given below,  $R_{GO} = \sqrt{(R_{Ob} \cos b)^2 + R_{Sun}^2 - 2 R_{Ob} \times R_{Sun} \cos l \cos b}$ , in which  $R_{Sun} = 8.5$  kpc is the Galactiocentric distance of Sun from the galactic center.

#### 4.6. Sensitivity

A measure of the weakest signal is discernible by a detecting system. The ratio of the amplitude of a signal above the noise level to the amplitude of the noise level itself is known as the signal-to-noise ratio. For most purposes, a minimum signal-to noise ratio of 1: 1 is required for the signal to be regarded as definitely detected. In the radio and infrared regions, the use of techniques such as integration, chopping, comparison with a stable laboratory source, and phase sensitive detection can improve the basic sensitivity of the system by several orders of magnitude.

### V. Summary

The discussed databases are the fundamental pillars of the modern astronomy. Moreover, these are effectively reducing the consumption of the time for scientific work in the field of astronomy. The CCD camera is effective tool to capture the emitted radiation of the stars. Present manuscript is also prescribed the summary of astronomical routines, which are applicable to estimate the stellar standard magnitudes. The prescribed

routines are performed through the various task of the IRAF and DAOPHOT software. In short, we have prescribed the astronomical web-infrastructure, which is a result of works of decades. Such services allow to us to do research work with easier and scientific way.

### Acknowledgment

GCJ is thankful to AP Cyber Zone (Nanakmatta) for providing computer facilities. GCJ is also thankful to Shree Nilamber Joshi for providing the friendly environment in the present working place, which becomes a milestone of my research work.

### References

- [1]. Albrecht M.A., Brighton A., Herlin T., et al., 1997, in *Astronomical Data Analysis Software and Systems VI*, ASP Conf. Ser. 125, 333
- [2]. Bessell, Michael S., 2000, *The Publications of the Astronomical Society of the Pacific (PASP)*, 112, 773, 961
- [3]. Bonatto, Ch., Bica, E. 2003, *A&A*, 405, 525
- [4]. Bonnarel F., Fernique P., Bienayme O., Egret D., Genova F., LouysM., Ochsenbein F., Wenger, M. and Bartlett J.G. 1991, *CCD astronomy. Construction and use of an astronomical CCD camera*, ed. Buil, C. 35
- [5]. Buonanno, R. & Iannicola, G., 1989, *Publ. Astron. Soc. Pac.*, 101, 294.
- [6]. Burt, D. J., "Basic operations of the Charge Couple devices". International conference on technology and application of the charge couple devices, September 1974, Edington: UNiversity of Edinburgh, center for industrial consultancy and liaison, 1974.
- [7]. Carpenter, J. M. 2001, *AJ*, 121, 2851
- [8]. Chromey, F. & Hasselbacher, D. A., 1996, *Publ. Astron. Soc. Pac.*, 108, 944.
- [9]. Cohen, Martin; Wheaton, Wm. A.; Megeath, S. T., 2003, *AJ*, 126, 1090
- [10]. De Medeiros, J. R., Ferreira Lopes, C. E., Leao, I. C., et al. 2013, *A&A*, 555, A63
- [11]. Florentin-Nielsen, R., Anderson, M., & Nielsen, S., 1995, in *New Developments in Array Technology and Applications*, eds. A. G. D. Philip, K. A. Janes, & A. R. Upgren, Kluwer, p. 207.
- [12]. Genova F., Egret D., Bienayme O., et al., 2000, *A&A* 143, 1
- [13]. Gilliland, R., 1992, in *Astronomical CCD Observing and Reduction Techniques*, ASP Conference Series Vol. 23, ed. S. Howell, p. 68.
- [14]. Ginsparg, P., 2011. "It was twenty years ago today". arXiv:1108.2700 [cs.DL]. Ginsparg, P., 2006, *Journal of Neuroscience* 26(38), 9606
- [15]. Greechie, R.; Pulmannova, S.; Svozil, K., 2005, *International Journal of Theoretical Physics* 44 (7), 691
- [16]. Hardie R.H., 1962, in *Astronomical Techniques* (ed. Hiltner W.A.) p.: 178.
- [17]. Harwit, M., 2006, *Astrophysical concepts* (Fourth edition), Springer Science +Business Media, LLC, p.: 1.
- [18]. Holtzman, J. A., 1990, *Publ. Astron. Soc. Pac.*, 102, 806.
- [19]. Howell, S. B., Koehn, B., Bowell, E. L. G., & Hoffman, M., 1996, *Astron. J.*, 112, 1302.
- [20]. Howell, S. B., et al., 2005, *Publ. Astron. Soc. Pac.*, 117, Nov Issue. Howell, S. B., 2006, *Handbook of CCD astronomy*, Second edition, Cambridge University Press, pp.2.
- [21]. Huber, D., Ireland, M. J., Bedding, T. R., et al. 2012, *ApJ*, 760, 32
- [22]. Jackson, A., 2002, *Notices of the American Mathematical Society* 49(1), 23
- [23]. Janesick, J. & Blouke, M., 1987, *Sky and Telescope Magazine*, September, 74, 238.
- [24]. Jaschek C., 1989, *Data in Astronomy*. Cambridge Univ. Press Khalaj, P., Baumgardt, H., 2013, *MNRAS*, 434, 3236
- [25]. Kristian, Jerome and Morley Blouke., 1982, *Scientific American*, 247(4), 66
- [26]. Kurtz, M.J.; Eichhorn G.; Accomazzi A.; Grant C.S.; Murray S.S.; Watson J.M., 2000, *Astronomy and Astrophysics Supplement*, 143(1), 41
- [27]. Kurtz, M.J.; Eichhorn G.; Accomazzi A.; Grant C.S.; Demleitner M.; Murray S.S., 2005, *The Journal of the American Society for Information Science and Technology*, 56(1), 36
- [28]. Landolt, A. U. 1992, *AJ*, 104, 304
- [29]. Massey, P. & Jacoby, G., 1992, in *Astronomical CCD Observing and Reduction Techniques*, ASP Conference Series Vol. 23, ed. S. Howell, p. 240.
- [30]. McKinney, Michelle (2011), "arXiv.org", *Reference Reviews* 25 (7): 3536, doi:10.1108/09504121111168622
- [31]. Merline, W. & Howell, S. B., 1995, *Exp. Astron.*, 6, 163.
- [32]. Mermilliod, J.-C., & Paunzen, E. 2003, *A&A*, 410, 511
- [33]. Monet, D. G., et al. 2003, *AJ*, 125, 984
- [34]. Mortara, L. & Fowler, A., 1981, in *Solid State Imagers for Astronomy*, Proc. SPIE, 290, 28.
- [35]. O'Connell, Heath (2000). "Physicists Thriving with Paperless Publishing". arXiv:physics/0007040.
- [36]. Ochsenbein F., 1982, in *Automated Data Retrieval in Astronomy*, Jaschek C. & Heintz W.D. (eds.), IAU Coll. 64. Dordrecht, D. Reidel Publishing Company, p. 171 (BSI)
- [37]. Ochsenbein F., Bauer P., Marcout J., 2000, *A&AS* 143, 23 (VizieR)
- [38]. Ochsenbein F., Bischoff M., Egret D., 1981, *A&AS* 43, 259 (CSI)
- [39]. Ochsenbein F., Dubois P., 1992, in *Astronomy from Large Databases, II*, Heck A. & Murtagh F. (eds.), p. 405
- [40]. Paz-Chinchon, F., Leão, I. C., Bravo, J. P., et al. 2015, *ArXiv e-prints* Persson, S. E., Murphy, D. C., Krzeminski, W., Roth, M., & Rieke, M. J. 1998, *AJ*, 116, 2475
- [41]. Roßner, S., Demleitner, M. & Schilbach, E., 2010, *AJ*, 139, 2440
- [42]. Sagar R., 1987, *BASI* 15, 193.
- [43]. Skrutskie, M. F., et al., 2006, *AJ*, 131, 1163
- [44]. Staff (January 13, 2015). "In the News: Open Access Journals". *Drug Discovery & Development*. Stetson P. B., 1987, *PASP*, 99, 191.
- [45]. Stetson, P. B. 1989, *Highlights of Astronomy*, 8, 635 40

- [46]. Stetson, P. B., Davis, L. E., & Crabtree, D. R., 1990, in *CCDs in Astronomy*, ASP Conference Series Vol. 8, ed. G. H. Jacoby, p. 289. Stetson P. B., 1992, *adass*, 1, 297.
- [47]. Tadross, A. L., 2011, *JKAS*, 44, 1 Tobin, W., 1993, in *Stellar Photometry Current Techniques and Future Developments*, eds. C. J. Butler & I. Elliott, IAU Colloquium 136, Cambridge University Press, p. 304.
- [48]. Tonry, J., et al., 2005, *Publ. Astron. Soc. Pac.*, 117, 281.
- [49]. Vence, Tracy (December 29, 2014), “One Million Preprints and Counting: A conversation with arXiv founder Paul Ginsparg”, *The Scientist*. Walkowicz, L. M. & Basri, G. S. 2013, *MNRAS*, 436, 1883
- [50]. Weisner and David E., “Charged-Coupled Devices”. McGraw-Hill Encyclopedia of science and Technology, 7th ed., McGraw Hill Inc.: New York, 1992.
- [51]. Wenger M., Ochsenein F., Egret D., Dubois P., Bonnarel F., Borde S., Genova F., Jasniewicz G., Laloe S., Lesteven S., and R. Monier, 2000, *Astron. Astrophys. Suppl. Ser.* 143, 9
- [52]. Wright, E. L., Eisenhardt, P. R. M., Mainzer, A. K., et al. 2010, *AJ*, 140, 1868
- [53]. Wu, Zhen-Yu., Ma, Jun., & Zhou, Xu. 2011, *PAPS*, 123, pp. 1313
- [54]. Zacharias, N., Finch, C. T., Girard, T. M., Henden, A., Bartlett, J. L., Monet, D. G., & Zacharias, M. I. 2013, *AJ*, 145, 44
- [55]. Zejda, M., Paunzen, E., Baumann, B., Mikulasek, Z. & Liska, 2012, *A&A*, 548, A97
- [56]. Zhou, X., et al., 2004, *A. J.*, 127, 3642.